

AD-750 896

FIZIKO-KHIMICHESKAYA MEKHANIKA MATERIALOV,
NUMBER 7, 1971 (SELECTED TRANSLATIONS).
SOVIET MATERIALS SCIENCE

Naval Intelligence Support Center
Washington, D. C.

28 September 1972

DISTRIBUTED BY:

NTIS

National Technical Information Service
U. S. DEPARTMENT OF COMMERCE
5285 Port Royal Road, Springfield Va. 22151



DEPARTMENT OF THE NAVY
NAVAL INTELLIGENCE SUPPORT CENTER
TRANSLATION SERVICES DIVISION
4301 SUITLAND ROAD
WASHINGTON, D. C. 20390

AD 750896

CLASSIFICATION:

UNCLASSIFIED

APPROVED FOR PUBLIC RELEASE, DISTRIBUTION UNLIMITED

TITLE:

Fiziko-khimicheskaya mekhanika materialov, No. 7, 1971
(Selected Translations)
Soviet Materials Science

AUTHOR(S):

Various

PAGES:

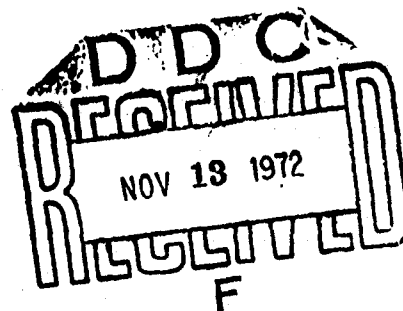
19

SOURCES:

Fiziko-khimicheskaya mekhanika materialov, No. 7, 1971
Pages 10-13; 13-15; 18-21; 87-89; and 89-91

ORIGINAL LANGUAGE:

Russian



TRANSLATOR:

C

NISC TRANSLATION NO.

3343

APPROVED

C.F.K.

DATE

28 September 1972

Reproduced by
NATIONAL TECHNICAL
INFORMATION SERVICE
U S Department of Commerce
Springfield VA 22151

DISTRIBUTION STATEMENT A

Approved for public release;
Distribution Unlimited

20 R

EFFECT OF THE BARRIER LAYER ON CERTAIN PROPERTIES

OF ALUMINIZED MEDIUM CARBON STEEL

[Article by V. I. Pokhmurskiy and V.S. Pikh (Institute of Physics and Mechanics, Academy of Sciences Ukrainian SSR, L'vov, Fiziko-khimicheskaya mekhanika materialov, Russian, No. 7, 1971, pp. 10-13]

/10*

One of the drawbacks of diffusion coatings on steels and alloys lies in their fairly low stability at high temperatures, which is caused by the chemical interaction of the coating material with the environment, sublimation of the saturating component, and the so-called dissipation of the diffusion layer. The phenomenon of dissipation, i.e. diffusion of the saturating component from the protective layer toward the interior of the parent metal is very frequently observed in aluminized steel generally operated at high temperatures. Dissipation of the layer leads to marked decrease of aluminum concentration on the surface of the part and hence to the deterioration of the protective properties of the coating. To enhance the high-temperature stability of aluminum coatings, the steel is coated -- prior to aluminizing -- with a barrier layer that inhibits the process of aluminum diffusion into the base metal. To produce a barrier layer, use could be made of nickel [1], which has low diffusion mobility in iron and fairly low interdiffusion with aluminum. The study included the effect of a barrier nickel layer on the high-temperature stability of an aluminized layer as well as on the creep of aluminized medium-carbon steel over a wide temperature range.

The barrier layers, 0.005 mm thick, were produced by the galvanic deposition of nickel on the specimens. To ensure reliable cohesion of the nickel layer with the base metal, the specimens were diffusion-annealed in argon at 1100°C for five hours. The structure was reduced by normalizing combined with saturation. The aluminizing was done from a powder mixture [2] in unsealed containers at 850°C for one hour.

It was found that the fine layer of nickel applied to medium-carbon steel prior to aluminizing effects a more uniform and high-grade diffusion coating. Its thickness, however, is about one half of that for aluminizing steel without nickel (Figure 1). Aluminum saturation of nickel specimens that had not been given diffusion annealing led to deterioration of the quality of the aluminized layer.

* Numbers in the margin indicate pagination in the original foreign text.

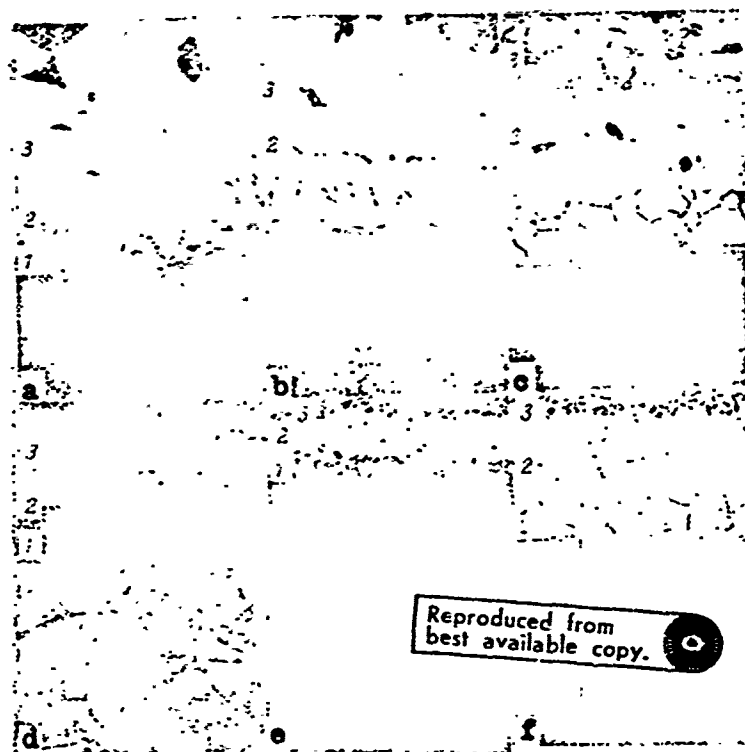


Figure 1. Microstructure (x 200) of aluminized 45 steel without a barrier layer (a,b,c), and with a barrier layer (d,e,f):
 a,d -- without diffusion annealing; b,e -- after diffusion annealing at 900 C, 2 hours; c,f -- the same, 8 hours.

Since nickel diffusion into the base metal during annealing is insignificant, the surface of the steel specimen retains a layer that is all-nickel. The aluminizing of such specimens entails the formation of various intermetallic compounds of nickel with aluminum; the properties of the diffusion layer will, therefore, vary with the depth of the layer, a situation manifested by marked distinctions in the microhardness of individual zones of the layer. The zone with the highest aluminum content (zone 3, Figure 1c) showed the highest microhardness value (750 kg/mm²). The deeper the layer within the specimen, the greater is the decrease in the aluminum content and the microhardness which drops down as low as 150 kg/mm² (zone 1, Figure 1e). There are also marked distinctions between the properties of diffusion layers produced on specimens with and without nickel. The maximum microhardness of diffusion layer produced on the steel without nickel is about 680 kg/mm².

/12

The aluminized layer on 45 steel without the barrier coating consists of three zones: zone 1 -- a solid solution with segregations primarily along the grain boundaries of the second phase; zone 2 -- needle-shaped inclusions of Fe₃Al and FeAl phases; zone 3 -- FeAl₂, Fe₂Al₅ and other similar aluminum-rich intermetallic compounds [1,3,4].

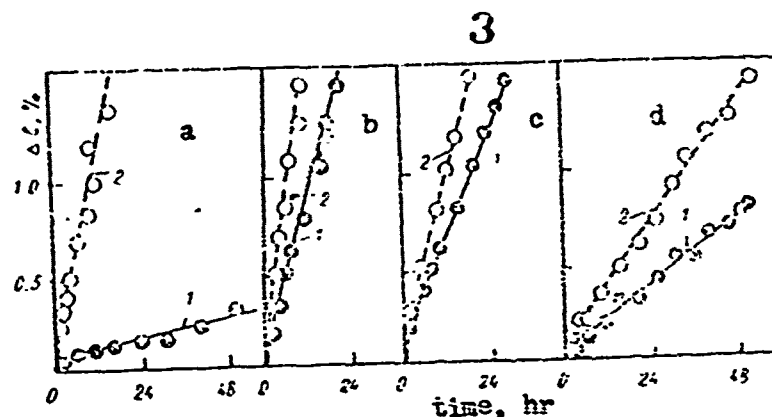


Figure 2. Creep curves of 45 aluminized steel with a barrier nickel layer (1) and without one (2):

a -- 450 C, $\sigma = 20 \text{ kg/mm}^2$; b -- 550 C, 9 kg/mm^2 ; c -- 650 C, 3.5 kg/mm^2 ; d -- 800 C, $\sigma = 0.63 \text{ kg/mm}^2$.

No study has been made of the structure of the aluminized layer on nickel-coated steel. It may be suggested that its first zone is made up of a solid solution of iron in nickel, the second, most probably of complex compounds of nickel-aluminum-iron, and the third zone consists of aluminum-nickel compounds (NiAl , Ni_2Al_3 ,) [5] (Figure 1d).

Subsequent heating of aluminized steel to 900°C and higher leads to significant changes in the diffusion layers, consisting of greater total thickness, primarily of the first zone containing least amounts of aluminum in the layer (Fig. 1a, b, c). As the diffusion layer dissipates, its microhardness decreases. The dissipation intensity increases with temperature. The nickel barrier layer markedly inhibits the dissipation process in the aluminized layer (Fig. 1d, e, f). The thickness of the diffusion layer in aluminized steel with a barrier nickel coating is less than that of steel without nickel; it is 15% less after a 2-hour anneal and 20% less after a 20-hr anneal (at 900°C).

The creep tests were conducted on R1-5 stress relaxation machines in an open atmosphere with specimens 10mm in diameter and 100-mm long working areas. The creep curves (Figure 2) show that the barrier nickel layer treated at the above temperatures markedly reduces the creep rate of aluminized medium-carbon steel.

The data obtained led to the conclusion that the barrier-type nickel layer on aluminized steel substantially reduces the dissipation of diffusion coatings, thus increasing their protective properties and also decreasing the creep of aluminized medium-carbon steel.

/ 13

REFERENCES

1. Minkevich, A.N. Khimiko-termicheskaya obrabotka metallov i spлавov (Chemical and Thermal Treatment of Metals and Alloys), "Mashinostroyeniye" Press, 1965.
2. Zamikhorskiy, V.A., Pokhmurskiy, V.I. and G. V. Karpenko. FKhMM, No. 6, 1966.

3. Karpenko, G.V., Pokhmurskiy, V.I. et al, Vliyaniye diffuzionnykh pokrytiy na prochnost' stal'nykh izdeliy (Effect of Diffusion Coatings on the Strength of Steel Products), "Naukova Dumka" Press, 1971.
4. Dekhtyar, M.V. SC. "Uporyadocheniye atomov i yego vliyaniye na svoystva splavov", (Collection: Ordering of Atoms and Its Effect on the Properties of Alloys), "Naukova dumka" Press, 1968.
5. Konstantinov, V.A. et al. 3b. "Zharostoykiye teplostoykiye pokrytiya" (Collection: Heat-Resistant and Thermostable Coatings), "Nauka" Press, 1969.

EFFECT OF ELECTROMECHANICAL HARDENING ON RESISTANCE
OF DRILL PIPES TO CORROSION FATIGUE FAILURE', → 8

/Article of G. V. Karpenko, A. M. Prishlyak, N. A. Severinchik and R. G. Pogoretskiy (Institute of Physics and Mechanics, Academy of Sciences Ukrainian SSR, L'vov; Institute of Petroleum and Gas, Ivano-Frankovo), Fiziko-khimicheskaya mekhanika materialov, Russian, No. 7, 1971, pp. 13-15/

The weakest component of the drilling string and the one most prone to failures is the threaded portion of the pipe /1,7. In the process of machine threading, the thread surface of the pipes generally shows some roughness and tear. The failure of drill pipes is, as a rule, the result of initiation and development of fatigue cracks from the surface of the tread. The quality of the surface layer of the thread is, therefore, the controlling factor for both the strength and productivity of drill pipes. /13*

The working capacity of drill pipes is usually increased by better pipe joint design, by, for example, welding the joints onto the pipes or using so-called blocking locks /2,3/. These methods, however, have some drawbacks. At present these locks cannot be welded to pipes classed under "E," "L," "M" strength groups on account of their poor weldability. Besides, the lock wears rather rapidly, which necessitates its rejection, as well as the pipe, although the latter is still serviceable. To enhance the carrying capacity and service life of pipes, electromechanical hardening of the pipe thread was used in this study, a method that can be readily applied at any repair shop in the petroleum industry.

Electromechanical hardening is a version of thermomechanical treatment of metals (TTM). The method is based on combining heating with the mechanical action of the tool for application to the surface layer of the part to be treated. The essence of this treatment lies in passing high-power current through the contact area of the tool; the metal becomes extremely hot and readily deforms and flattens under the pressure of the tool. The pressure, pulsed heating and rapid cooling through the heat transfer toward the metal's interior results in hardening and the emergence of a unique structure of white layers /4,5/. /14

The electromechanical hardening of the threaded portion of drill pipes (D-strength group), 114mm in diameter was conducted on 1983M pipe-threading machines. The working section of the planishing tool was made from T15k6 hard alloy. Better hardening results of the thread surface were obtained with current intensities of 400-450 amp and 3.5-4 v.

*Numbers in the margin indicate pagination in the original foreign text

The tests indicate that electromechanical hardening attains maximum effectiveness in 2-3 passes at $v = 0.35$ m/sec, which means that the surface finish meets class 8-9 (GOST 2789-59). Increasing the number of passes impairs the surface finish due to the tempering of the hardened layer and scaling.

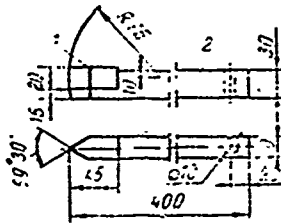


Fig. 1. Design of the planishing tool; 1--hard alloy; 2--holder.

Fatigue tests of drill pipes in corrosive media* were conducted by bending the specimen through an angle and rotating at 730 rpm $\overline{1}$.

Analysis of data on the corrosion-fatigue strength of nonhardened drill pipes indicates their arbitrary fatigue limit on the basis of 10^7 cycles to be 7 kg/mm^2 (Fig. 2). The low corrosion-fatigue strength of the pipes is attributed to high stress concentration caused by the thread, cyclic friction in the pipe-joint pair, and crevice corrosion in the threaded joint.

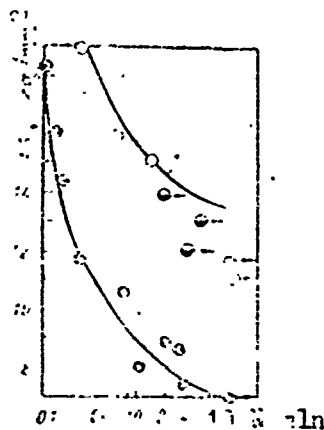


Fig. 2. Corrosion-fatigue curves for drill pipes: 1--commercial-type pipes; 2--Pipes after electromechanical hardening (* breakdown in the pipe outside the thread)

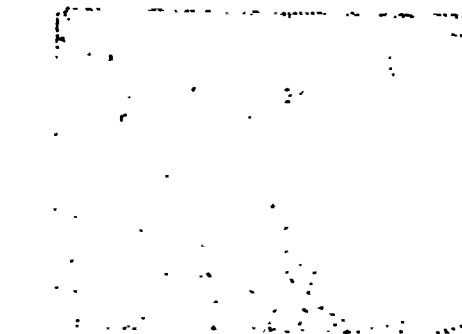


Fig. 3. Microstructure (X200) of the surface layer after electromechanical treatment, tested for corrosion fatigue in drilling mud ($\sigma = 12 \text{ kg/mm}^2$; $N = 3.50$ million cycles)

Electromechanical treatment of the threaded portion of drill pipes markedly increases their corrosion fatigue strength (Fig. 2). It should

*The settled drilling mud of Dolina oil fields, Ivano-Frankovo oblast $\overline{1}$ served as the corrosive medium.

be noted that stresses of $14-12\text{kg/mm}^2$ failed to cause thread damage; all breakdowns occurred along the body of the pipe at distances ranging from 100-150mm from the end of the thread.* Because of this, the exact fatigue limit of the hardened pipes on the basis of 10^7 cycles could not be determined; there is every reason to assume, however, that the limit could be raised by electromechanical hardening by about a factor of 2. In practice, pipe breakdowns (the body) occur rather rarely; therefore, hardening the thread by electromechanical treatment is bound to raise significantly the efficiency of drilling as a whole.

/15

The increase in the corrosion-fatigue strength of drill pipes following electromechanical treatment is attributed to changes in the physicomachanical properties of the thread's surface layer: the surface finish is upgraded by 3-4 classes, and the structure of the surface layer is markedly refined (Fig. 3), its microhardness up to 0.1mm in depth increasing about threefold. As a result, the surface layer acquires better physical and mechanical properties that enhance its resistivity to the action of external aggressive media.

REFERENCES

1. Severinchik, N. A., Karpenko, G. V., Pogoretskiy, R. G. and A. M. Prishlyak, FKhMM, No. 4, 1971.
2. Erlich, G. M. Ekspluatatsiya buriľnykh trub (Operation of Drill Pipes), "Nedra" Press, 1969.
3. Pivovarov, I. F., Sarosyan, A. Ye., Shcherbyuk, N. D. et al. Spravochnoye rukovodstvo po neftepromyslovym trubam (Handbook for Oil Drill Pipes), "Nedra" Press, 1967.
4. Askinazi, B. M. Uprochneniye i vosstanovleniye detaley elektromekhanicheskoy obrabotkoy (Hardening and Restoration of Parts by Electromechanical (Hardening). "Mashinostroyeniye" Press, 1968.
5. Karpenko, G. V., Babey, Yu. I., Karpenko, I. V. and E. M. Gutman. Uprochneniye stal' mekhanicheskoy obrabotkoy (Hardening of Steel by Mechanical Treatment). "Naukova Dumka" Press, 1966.

* Ultrasonic flaw detection failed to find any cracks in the threaded portion.

CORROSION-CRACK TRAJECTORY IN BIAxIAL PLANE
STATE OF STRESS)

[Article by O. I. Steklov (Moscow Higher Technical School imeni N. E. Bauman), Fiziko-khimicheskaya mekhanika materialov, Russian, No 7, 1971, pp 18-21]

Crack trajectories and stress components controlling the crack path in corrosion cracking have been the topic of a number of earlier papers. Stresses were produced in specimens through uniaxial loading, primarily by stretching, compression, bending, and torsion. Analysis of these papers [1] indicates that corrosion cracks are caused by tensile stress components regardless of the method of loading. /18*

Most structures operated in aggressive media are shell shaped (tanks, pipelines) and feature biaxial plane state of stress. Of interest here are factors acting on the corrosion crack trajectory under such a state of stress.

The investigations were conducted on disk-shaped specimens in which two-dimensional biaxial state of stress was produced by welding [2]. The circular weld joints were symmetric to the center of the specimens. The heat deformation effect of welding produced in the specimens a biaxial axisymmetric field of residual welding stresses, of which the principal stress components are tangential σ_t and radial σ_r stresses. Varying the diameter of the circular weld joint is likely to produce various stressed states: from a rigid biaxial system for small diameters to a nearly uniaxial system for large diameters (Fig. 1).

The test involved OT4 titanium alloy specimens including Kh18N10T and St.3sp steel specimens. To eliminate chemical and metallurgical effects, the welding was conducted in a neutral atmosphere (A-grade argon) with a nonconsumable tungsten electrode under conditions affording a quality joint. The titanium specimens were tested in a bromine-methanol medium in which titanium is susceptible to intensive corrosion cracking [3]. By varying the bromine, methyl alcohol, and water contents it is possible to regulate the time interval before corrosion cracking over a range from several minutes to thousands of hours. This study made use of a BM2.5-5 solution (2.5% Br, 5% H₂O and the balance methanol) in which the susceptibility of the weld joint to corrosion was close to that of the parent metal; this compensates, to some extent, for the inhomogeneity of proper- /19

* Numbers in the margin indicate pagination of the original foreign text /20

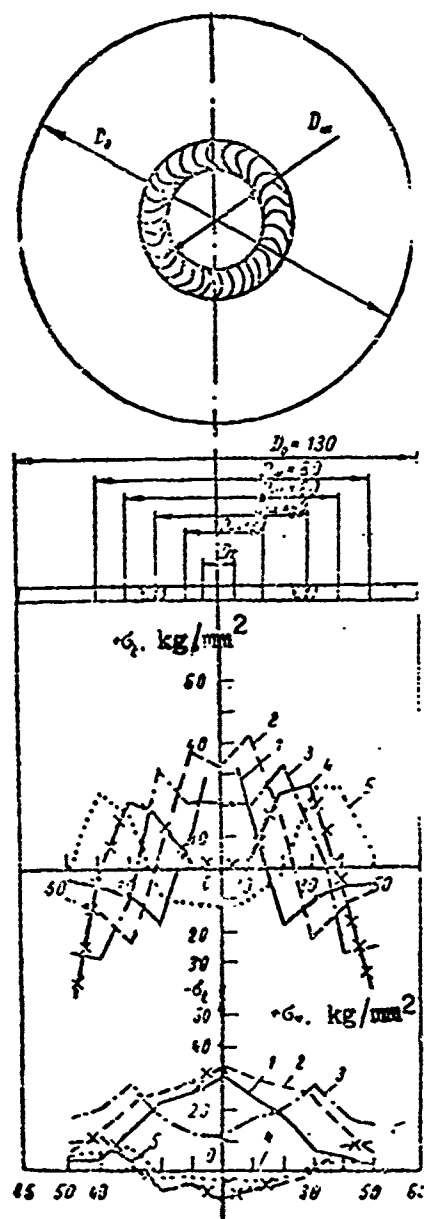


Fig. 1. Effect of the diameter of the circular weld on the magnitude and distribution of residual tangential σ_t and radial σ_r stresses in a OT4 titanium alloy specimen: 1-- $D_w=15$ mm; 2-- $D_w=20$ mm; 3-- $D_w=40$ mm; 4-- $D_w=60$ mm; 5-- $D_w=80$ mm.

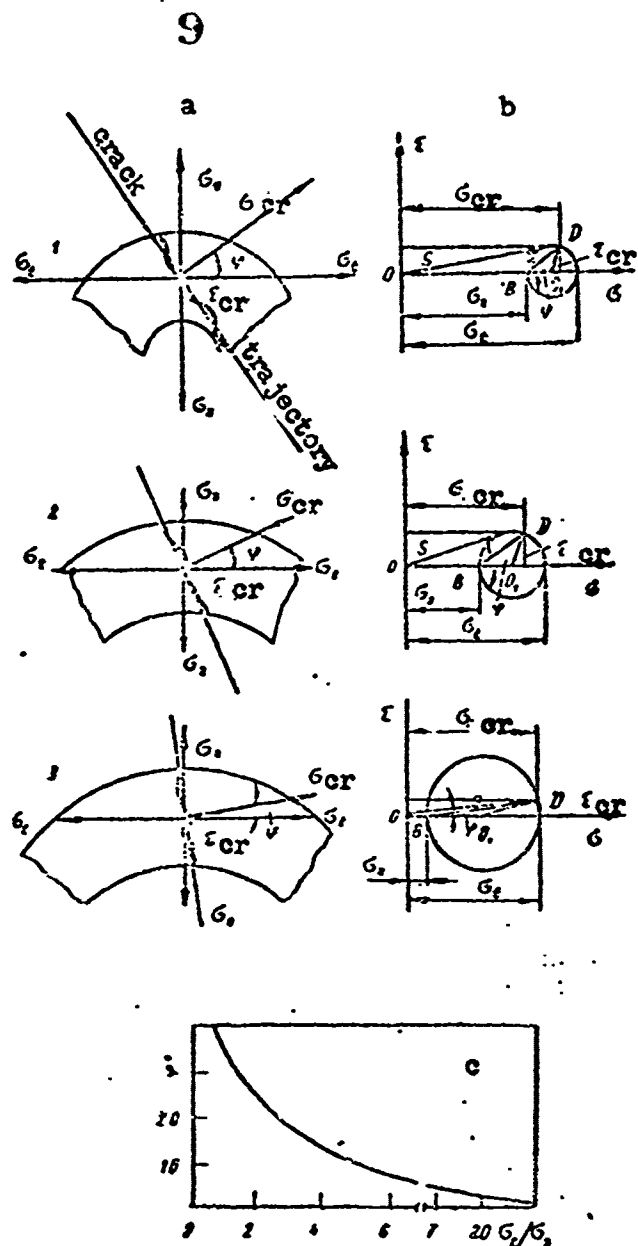


Fig. 2. Analysis of stressed state and crack trajectory in biaxial stress. Disk specimens, 130 mm in diameter, weld diameter — 20 mm (1), 40 mm (2), 80 mm (3): a) stress state and crack path; b) Mohr diagram; c) angle φ between the normal to the crack trajectory and the principal normal stress as a function of rigidity of the stress diagram (σ_t/σ_r)

ties produced by welding. The Kh18Ni10T steel specimens were tested in a boiling saturated solution of $MgCl_2$ and those of St.3sp steel in a boiling solution of nitrates -- 45% by weight $Ca(NO_3)_2$ + 35% by weight NH_4NO_3 .

In the first approximation, involving the classical theories of strength, it is assumed that the corrosion crack trajectory is determined by the values and distribution of stresses existing in the body without cracks. To analyze the state of stress in the crack zone, Mohr's stress diagram was used. As known from earlier research [4], this diagram, is plotted by drawing inter-perpendicular axes σ_n and τ and assigning points whose coordinates are equal to stresses acting on the principal stress platforms (for this state of stress the principal stresses being tangential σ_t and radial σ_r , Fig. 2). Any point D of the circumference plotted on the segment BA which is equal to the difference $\sigma_{\max} - \sigma_{\min}$ has two coordinates equal to the normal and tangential stresses σ_n and τ_n on an inclined platform whose normal to the direction of the highest principal stress σ_{\max} forms an angle φ . This angle φ is formed between the axis σ_n and the straight line connecting point B on the circumference with point D. If the component in which the stresses are studied is plotted so that the greater stress $\sigma_{\max} - \sigma_t$ is parallel with axis σ_n , then the line BD will be parallel to the normal \bar{n} to the platform on which stresses σ_n and τ_n are equal to coordinates of point D. Segment OD provides the value of total stress S_n on the platform with angle

Диаметр шва, мм (1)	σ_t , кг/мм ² (2)	σ_r , кг/мм ² (3)	σ_t/σ_r (4)	φ , град (5)	σ_{CR} (6)	τ_{CR} (7)	S_{CR} (8)	σ_i (9)	τ_{\max} (10)	Время до растрескивания, ч (11)
					кг/мм ² (12)					
20	39.3	28.6	1.38	33.5	36	5	36.5	35.2	5.4	9
40	30.4	16.6	1.83	25	27	5.7	28	28.5	7.9	18
80	29.9	3.8	7.8	6	23.5	2.5	29.8	27.3	13	224

Note: Commas represent decimal points

Legend: 1--weld diameter, mm; 2-- σ_t , kg/mm²; 3-- σ_r , kg/mm²; 4-- σ_t/σ_r ; 5-- , deg.; 6-- σ_{CR} ; 7-- τ_{CR} ; 8-- S_{CR} ; 9-- σ_i ; 10-- τ_{\max} ; 11--time before cracking, hr; 12--kg/mm².

The disc specimens were built up with axisymmetric circular welds of various diameters to create stressed states with various principal stress ratios, i.e., $\sigma_{\max}/\sigma_{\min} = \sigma_t/\sigma_r \approx 1$ to 20, and to correlate the stressed state in the weld metal with the nature of stress propagation. The results of the analysis for the cast weld metal are cited in Fig. 2, where σ_t , σ_r are the respective values of the principal tangential and radial stress components in the experimental weld, and φ is the angle between

the direction of the principal stress component coinciding with axis σ_n in fig. 2 and the normal to the crack trajectory in the weld. The angle φ was plotted directly on the specimens; σ_{CR} is the normal stress perpendicular to the crack trajectory (plotted according to Mohr's diagram); τ_{CR} is the tangential stress parallel to the crack trajectory (based on Mohr's diagram); S_{CR} is the total stress in the crack zone (also based on Mohr's diagram); $\sigma_i = \sqrt{\sigma_t^2 - \sigma_t \sigma_r + \sigma_r^2}$ is the equivalent (reduced) stress in the biaxial stressed state according to the power theory of strength (deformation theory); $\tau_{\max} = (\sigma_{\max} - \sigma_{\min})/2 = (\sigma_t - \sigma_r)/2$ is the highest tangential stress acting on the platform and dividing in half the angle between the maximum and minimum principal stresses, i.e. at 45° angle to direction σ_t .

The analysis of the state of stress and the correlation of the nature of its propagation implies the following: a) The normal tensile stress in the plane of the crack which is the equivalent resultant of principal stresses serves as the stress component that causes cracking and governs the crack trajectory under conditions of biaxial plane state of stress; b) The angle φ between the normal to the crack and the highest principal stress σ_t is a function of the principal stress ratio σ_t/σ_r . The equivalent stress resultant that determines the crack trajectory approaches the maximum principal stress, with a decrease of the second stress component both in magnitude and direction. c) Tangential stresses are small compared with normal stresses. The crack trajectory does not coincide with the direction of maximum stresses τ_{\max} and, therefore, tangential stresses are not the factors controlling the trajectory. d) Increasing both the diagram's rigidity and the stresses promotes the process of cracking. e) The crack trajectory indirectly reflects the distribution of residual welding stress.

/21

The crack trajectory in the parent metal is also affected by the metal's anisotropy due to the presence of grain orientation caused by rolling. The crack develops primarily in the direction of rolling. Thus, if the metal contains zones with higher susceptibility to corrosive action, the arrangement of these zones becomes the significant, and sometimes the controlling, factor for the crack trajectory. For example, the inhomogeneity of plastic deformation in the weld joints of Kh18N10T steel predetermines the emergence and initial trajectory of the crack [5].

The above analysis leads to the following conclusions. In case the metal has uniform resistance to corrosive attacks, the crack trajectory under biaxial tensile stresses is determined by the tensile component normal to the crack's trajectory; this stress component is the equivalent resultant of the principal normal tensile stresses. In case the metal's resistance to corrosive attacks is nonuniform, the direction of crack propagation is determined by the combined effects of the equivalent resultant of the principal normal stress components and the arrangement of zones having higher susceptibility to the action of the corrosive medium.

Reproduced from
best available copy.

References

1. Romanov, V. V. Korrozionnoye rastreskivaniye metallov (Corrosion Cracking of Metals), Mashgiz, Moscow, 1960
2. Steklov, O. I. and A. I. Akulov. O vliyaniy ostatochnykh svarochnykh napryazheniy i vida napryazhennogo sostoyaniya na korrozionnoye rastreskivaniye svarnykh soyedineniy (Effect of Residual Welding Stresses and State of Stress on Corrosion Cracking of Weld Joints), 1965, No. 2.
3. Avtorskoye svidetel'stvo (Author's Certificate) No. 175697.
4. Spravochnik mashinostroitelya (Mechanical Engineer's Handbook), Mashgiz, Vol. 3, 1962.
5. Steklov, O. I. and Badayev, A. S. Svarochnoye proizvodstvo (Welding Production), No. 2, 1969.

EFFECT OF ANODIZING ON FATIGUE LIMIT AND CORROSION-
FATIGUE STRENGTH OF DURALUMINUM SHEETS WITH STRESS
CONCENTRATORS

[Article by A. V. Karlashov and A. G. Gaynutdinov (Kiev
Institute of Civil Aviation), Fiziko-khimicheskaya mekhanika
materialov, Russian, No. 7, 1971, pp. 87-89]

Until recently, research in anodizing was directed primarily towards determining the protective properties of anodic coatings under overstress [1,2]. The information available on the protective properties of these coatings under loads is rather limited, and that on the mechanism of protection under these conditions is practically nonexistent.

/87*

The papers published on the effects of anodic coatings on the corrosion-fatigue strength of aluminum alloys refer to experiments conducted on smooth specimens while real products have a multitude of stress concentrators of which the most commonly known are rivet holes. It would therefore be useful to investigate the effect of sulfuric acid anodizing on the fatigue limit and corrosion-fatigue strength of clad duraluminum sheets with stress concentrators.

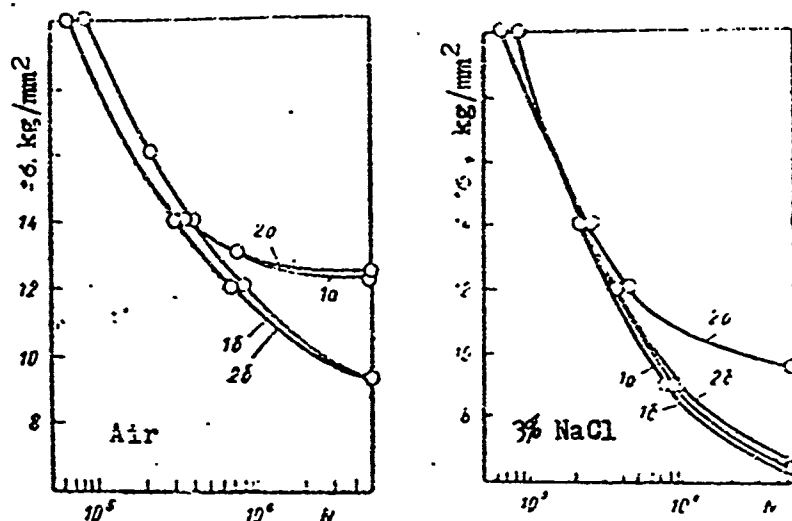
The study described here was conducted on flat specimens of D16AT alloy cut from a 2-mm sheet along the direction of rolling. The specifications of the anodizing procedure were as follows [1]: electrolyte, H_2SO_4 ; density, 1.84 kg/cm^3 ; concentration, 180 g/l; temperature, 20°C ; current density, 1 A/dm^2 ; anodizing time, 35 min. The thickness of the anodic coating was determined by weight at 9.1μ [1]. The coatings were condensed in boiling water for 25 min. The drilling and riveting were done after the specimens had been anodized under plant conditions using current technology. The fatigue tests of smooth specimens and those with riveted holes were conducted by pure symmetric bending. A 3% NaCl solution served as the corrosive medium. The results of the experimental study on the fatigue limits and corrosion fatigue strength of the specimens are reflected in the curves, shown on the following page, plotted for the probability of failure ($P = 50\%$) on the basis of averaged test data from 7-10 specimens at every stress level.

/88

Tests conducted in open air have shown that the effect of anodic coatings on the fatigue limits of both smooth and rivet-holed specimens is a function of stress level. At high stress levels, anodizing appears to reduce the fatigue limit while at low stress levels the fatigue limit is

*Numbers in the margin indicate pagination in the original foreign text

unaffected by anodizing. For example, for a test base of $5 \cdot 10^6$ cycles, the arbitrary fatigue limits of both anodized smooth specimens and rivet-holed specimens are practically the same as those of similar unprotected specimens.



Fatigue curves of smooth specimens (a) and specimens with rivet holes from D16AT duraluminum (b) from tests in open air and 3% solution of NaCl: 1—without coating; 2—with anodic film.

The tests conducted in a corrosive medium, similarly to open-air tests, indicate that the effect of anodic coatings is a function of stress level; it manifests itself, however, to a greater extent in the corrosive medium. For example, the arbitrary fatigue limit of anodized smooth specimens in the corrosive medium is 52% higher than the fatigue limit of unanodized smooth specimens. In the presence of stress concentrations the effectiveness of anodic coating is highly reduced: the arbitrary corrosion fatigue limit of specimens with riveted holes is only 6% higher than that of similar unanodized specimens, i.e., the corrosion fatigue limits of specimens with rivet holes are practically the same both before and after anodizing.

Thus, the effectiveness of anodic coatings under both fatigue and corrosion fatigue conditions at given stress levels is greatly reduced in the presence of stress concentrators (riveted holes).

Earlier research deals with compressive residual stresses that act within the anodic coating on a D16 alloy [3,4]. The effect of anodizing on the fatigue strength of the alloy both in air and corrosive media is attributed to the residual stresses in the coating and its shielding action as well as to stress concentrations in the cracks of the coating that appear

during cyclic application of stresses. The effect of anodizing on both the fatigue limits and corrosion-fatigue strength of uncladded duraluminum in the presence of stress concentrators (riveted holes) is slightly reduced even though the cylindrical surface of the holes under the rivets appears to be free from anodic coating as in the case of specimens of cladded sheet material [5]. In this connection one might theorize that fatigue cracks both in air and in corrosive media may be generated not on the cylindrical surface of the holes under the rivets but on the surface of the specimens in the rivet head area. The reason is that the material's fatigue limit at the cylindrical surface of the hole both in air and corrosive media is obviously higher than at the protected surface of the specimen because of the strengthening of the material by closing the rivet head and the elastic radial stress produced by the body of the rivet [6]. The nearly complete loss of the beneficial effect of anodizing on the fatigue limit of cladded specimens in air and corrosive media may then be attributed to the fact that the cladded layer (with its low mechanical properties) is completely crumpled by the impact of riveting and that the anodic coating at the rivet head is, as a result, destroyed. This assumption is supported by microscopic examinations. A survey of the specimen's surface in the rivet head area (after removal of the rivets) revealed a network of cracks in the anodic coating arranged both radially and along the periphery of the hole.

/89

The above study gives rise to the conclusion that the effect of anodic coatings on the fatigue limits and corrosion-fatigue strength of D16AT duraluminum is a function of stress level: at high stress levels anodizing decreases the material's fatigue limit in both open air and corrosive media but increases it at low stress levels. The beneficial effect of anodic coatings on the fatigue limit and corrosion fatigue strength of duraluminum is practically eliminated in the presence of stress concentrators.

REFERENCES

1. Golubev, A. I. Anodnoye okisleniye alyuminiyevykh splavov (Anodic Oxidation of Aluminum Alloys). Izd. AN SSSR, 1961.
2. Vernik, S. and R. Pinner. Khimicheskaya i elektrokhimicheskaya obrabotka alumiya i yego splavov (Chemical and Electrochemical Treatment of Aluminum and its Alloys) Sudpromgiz, 1960.
3. Karlashov, A. V. and R. G. Gaynutdinov. FKhM, 1970, No. 2.
4. Karlashov, A. V. and R. G. Gaynutdinov. FKhM, No. 5, 1970.
5. Karlashov, A. V., Gaynutdinov, R. G. and G. A. Stukanogov. K voprosu o roli anodnoy plenki pri korroziionnoy ustalosti obratstov dyuraluminiya D16T s kontsentratorami napryazheniya

(The Role of Anodic Coatings in Corrosion Fatigue of D16T Duraluminum Specimens with Stress Concentrators). Materialy Konferentsii (Proceedings of a Conference), Kiev, 1968.

6. Marin, N. I. Statisticheskaya vyнослиvost' elementov aviatsionnykh konstruktsiy (Static Strength of Elements of Aviation Structures), "Mashinostroyeniye" Press, 1968.

EFFECT OF STRUCTURE ON FATIGUE STRENGTH OF CERTAIN

TITANIUM ALLOYS,

[Article by V. A. Gladkovskiy, M. S. Nemanov and Yu. P. Sirin (Perm' Polytechnic Institute), Fiziko-khimicheskaya mekhanika materialov, Russian, No. 7, 1971, pp. 89-91/

Titanium alloys are the most promising materials for machine construction because of their low specific weight, high strength, fatigue characteristics and high corrosion resistance. For most of these alloys the fatigue-to-tensile strength ratio is about 0.50, i.e., close to that for steels of the ferrite-pearlite class. Yet the corrosive effect of the media in reducing the fatigue limit of titanium alloys is much lower than for the steels. The corrosion fatigue limit of VT-8 and VT3-1 titanium alloys given preliminary upgrading heat treatment was reduced only by 5 - 8% /1/. /89*

The fatigue strength of titanium alloys depends largely on the methods of producing the intermediate products (forging, rolling), heat treating, final surface finishing, i.e., the materials structure, and the magnitude and pattern of distribution of residual stress /2,4/.

The operating temperature during forging and rolling cannot be maintained constant; the semifinished products will, therefore, have considerable structural inhomogeneity both over the length and cross section of the billet.

The objective of these experiments was to determine the effect on fatigue strength in open air and corrosive media of the structural inhomogeneity of an AT-3 titanium alloy supplemented with aluminum (tensile strength = 81 - 86 kg/mm²; yield strength = 74 - 79.5 kg/mm²; elongation at rupture = 15 - 20.6%; reduction in area at rupture = 32 - 39%; HRC = 26 - 28; notch toughness = 7.7 - 8.2 kg/cm²). The tests were conducted on smooth specimens (GOST 2860-65), 10 mm in diameter, prepared from annealed forged plates (forging end temperature, 840 - 880 C). The specimens were produced by identical technology (they were fine layers of metal having been removed at the final passes). The working surface was finished by polishing to meet class 10 (GOST 278 - 56). /90

The fatigue tests in open air and corrosive media (3% NaCl solution) were done on tensile testing machines by bending through an angle with symmetric stress alternation applied to the rotating specimens. The test base in open air was 10⁷ and in corrosive media 3·10⁷ cycles. In all experiments 2000 rpm was used. The corrosion fatigue tests consisted of complete immersion of the specimens in the circulating corrosive medium. The solution was replaced every 10 days; no more than 6 specimens were tested at a time.

*Numbers in the margin indicate pagination in the original foreign text

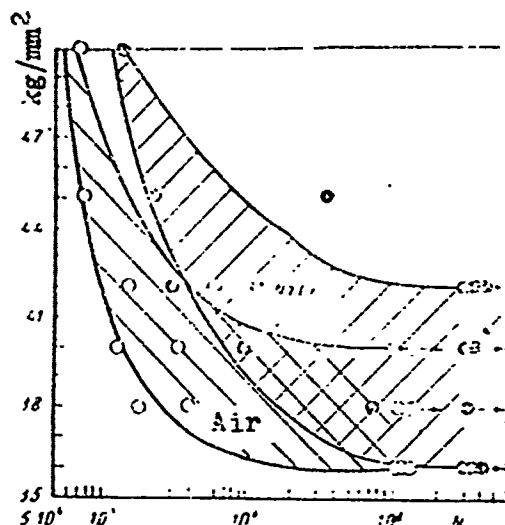


Fig. 1. Fatigue limit curves of the alloy.

As a rule, the specimens were not brought up to complete failure. A special machine-cutoff mechanism was set up to monitor the increase in the specimen's sag due to the development of cracks in the critical cross-section area. At the instant of critical sag and machine cutoff, the cracks covered about one half of the specimen's cross section. The fractures were revealed by static loading.

The tests have shown that the service life of specimens at high stress levels in a corrosive medium is slightly higher than in open air (Fig. 1). This was observed when the specimens were completely immersed in the circulating solution and the oxygen supply to their surface was hindered; intensive cooling of the specimens during the tests was also noted. Both open-air and corrosive media tests exhibited a wide variance of fatigue limit and service life values, which is largely attributed to the structural inhomogeneity of the material.

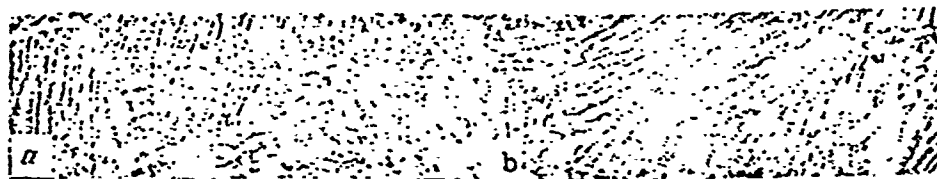


Fig. 2. Microstructure of the alloy (X100): a)—specimens with high fatigue strength; b)—specimen with low fatigue strength

Higher fatigue strength characteristics were found to coincide with a finer grain structure (Fig. 2). According to the microstructural scale for titanium alloys [5], the specimen's microstructure shown in Fig. 2a is the optimum one and it reflects high resistance to fatigue failure, while that in Fig. 2b represents a structure of overheating followed by a reduction of the mechanical properties of the alloy. A similar regularity was revealed for the corrosion-fatigue strength characteristics.

Thus, to obtain optimum fatigue strength values for AT-3 titanium alloys, attempts must be made to produce a material of fine homogeneous structure.

REFERENCES

1. Pokhmurskiy, V. I., Kulik, V. A. and G. V. Karpenku, FKhMM, No. 1, 1969.
2. Hempel, M., Draht, Vol. 16, No. 4, 1965, pp. 209-218.
3. Hempel, M., Draht, Vol. 17, No. 4, 1966, pp. 206-218.
4. Huffer, D. and W. Hofmann, Materialpruefung, Vol. 3, No. 1, 1961, pp. 5-14.
5. Glazunov, S. G. SC. "Titanovyye splavy dlya novoy tekhnologii
(Titanium Alloys for the New Technology), "Nauka" Press, 1968.